ELSEVIER

Ceramics International 26 (2000) 221–230

CERAMICS INTERNATIONAL

The effects of sintering temperature on the properties of hydroxyapatite

G. Muralithran, S. Ramesh*

Advanced Materials Research Centre (AMREC), SIRIM Berhad, 1 Persiaran Dato Menteri, PO Box 7035, 40911 Shah Alam, Malaysia

Received 6 May 1999; received in revised form 14 May 1999; accepted 14 June 1999

Abstract

The sintering behaviour of hydroxyapatite (HA), the resulting microstructure and properties are influenced not only by the characteristics and impurities of the raw materials but also were found to be dependent on the thermal history during the fabrication process. This work is concerned with the effects of grain size on the relative density and hardness. A commercially available HA powder was cold isostatically pressed at 200 MPa and sintered at temperatures ranging from 1000 to 1450°C with a dwell time of 2 hours. It has been found that, at the optimum sintering temperature of 1250°C where the material is composed of pure hydroxyapatite phase, the samples exhibited densities >99% of theoretical value and possessed a hardness value of 6.08 GPa. Decomposition of HA starts to occur at ~1400°C with the formation of TCP phase. The change in hardness was found to be dependent on the relative density up to a certain grain size limit. However, above this grain size limit, no correlation exists between the two properties. Porosity and grain size were found to play an important role in determining the properties of sintered hydroxyapatite compacts.

Keywords: Sintering; Properties; Hydroxyapatite

1. Introduction

Hydroxyapatite (HA) is sometimes referred to as calcium phosphate tribasic and has the chemical formula $Ca_{10}(PO_4)_6(OH)_2$. The material has received considerable attention over the past two decades as an implant material due to its excellent biocompatability [1, 2]. HA is a bioactive material mainly because of its calcium-to-phosphorus ratio being similar to that of natural bone and teeth, thus, rendering this material an ideal candidate for clinical applications either in the form of a fully dense sintered material [3] or as a coating material on a bioinert metallic implant [4,5].

Although HA is a promising implant material, its use under load bearing applications such as artificial joints have been restricted by the low toughness (0.8–1.2 MPa $m^{1/2}$) and low flexural strength (<140 MPa) of the ceramic body [6–8].

In order to improve the mechanical properties of sintered hydroxyapatite, the properties of the powder precursors have been studied by controlling important parameters such as particle size and shape, particle distribution and agglomeration [9]. The production of submicron HA powders is also being investigated as it exhibits greater surface area [10]. This in turn would provide improved sinterability and enhanced densification. Nanometer sized HA is also expected to have better bioactivity than coarser crystals [10,11]. The presence of hard agglomerates in the powder precursors have been found to exhibit a higher green density than the surrounding matrix [12,13]. As a result, during sintering, thermal gradient exists across the cross-sectional area of the compact and this would encourage differential densification to occur which would eventually lead to the formation of microstructural defects that limit the mechanical strength of the sintered body [14].

Another factor that is critical in the sintering behaviour of HA is the densification process which may be achieved by pressureless sintering, microwave sintering and hot-pressing. Densification of HA is usually achieved via compaction and sintering. Uni-axial pressing is the most common method of achieving compaction but the sintered body tends to lose its uniformity and develop cracks [15]. Hot-pressing of hydroxyapatite has been found to allow densification to take place at much lower temperatures than in the conventional sintering

* Corresponding author. Tel.: +60-3-556-7873; fax: +60-3-556-7867.

E-mail address: ramesh-singh@sirim.my (S. Ramesh).

0272-8842/00/$20.00
PII: S0272-8842(99)00046-2

process [16]. This is an advantage as a lower temperature of densification prevents the formation of other calcium phosphate phases such as α-TCP and β-TCP that may form when sintered at temperatures above 900°C [17].

The sintering temperature and atmosphere are also important as these factors could adversely affect the strength of HA. For instance, sintering at elevated temperatures has the tendency to eliminate the functional group OH in the HA matrix (dehydration) and this would result in the decomposition of HA phase to form α-tricalcium phosphate (α-TCP), β-tricalcium phosphate (β-TCP) and tetracalcium phosphate (TTCP) [18]. It is worth mentioning that decomposition of HA suppresses densification and will be accompanied by a decrease in mechanical properties [19].

The aim of the present work was to study the effects of sintering temperatures on the properties of cold-isostatically pressed commercial hydroxyapatite. The thermal stability of HA was assessed in terms of phases present, densification behaviour and hardness. In addition, the effects of porosity and grain size on the hardness of sintered HA were also investigated.

2. Experimental procedure

2.1. Powder characterisation

A commercially available hydroxyapatite powder (Merck 2196, Germany) was used for this work. In order to determine the calcium (Ca) content, the powder was dissolved in nitric acid and analysed by the inductively coupled plasma (ICP) method whereas the titration method of standard EDTA solution was used to determine the phosphate (P) content. Fourier transform infrared (FTIR) spectrum of the powder was obtained by using a Nicolet MAGMA 760 spectrometer. Prior to FTIR analyses, the powder was mixed with KBr and pressed into pellets. The phases present in the powder were identified by using a Rigaku D-MAX X-ray diffractometer with Cu-K_α radiation source at a scan speed of 0.5°/min and a step scan of 0.02°. Morphology of the powder precursor was also examined using a Philips XL40 scanning electron microscope (SEM). The particle size distribution of the powder was obtained using a Coulter laser particle size analyser with a sensitivity of 0.4 μm. Prior to this measurement, the powder was mixed in distilled water and treated in an ultrasonic bath for 10–15 min in order to break any agglomerates. In addition, specific surface area of the powder was also measured by the BET method.

2.2. Sample preparation

The HA powder was uniaxially pressed at 40 MPa into pellets using a 20 mm cylindrical die. The compacted green body was subsequently placed in a rubber bag and cold isostatically pressed (CIP) at 200 MPa. The CIP green samples exhibited a linear shrinkage of 10%. The CIP pellets were sintered in air at temperatures ranging from 1000 to 1450°C, at a furnace ramp rate of 2°C/min and soaking time of 2 h.

2.3. Characterisation of sintered body

The linear shrinkage of the fired samples was determined by comparing the difference in the diameter of the green body and sintered body. The density of the sintered samples was determined by Archimedes' method using distilled water. The relative density was obtained by taking the theoretical density of hydroxyapatite as 3.156 g cm^{-3}. The crystalline phases present in the samples were identified by X-ray diffraction (XRD) in reference to standard JCPDS cards available in the system software. In addition, microstructural evolution under the various sintering temperatures was examined using scanning electron microscopy (SEM). The samples were polished to 1 μm surface finish using diamond paste and subsequently etched with 0.5% HF to delineate the grain boundaries. The average grain size was determined from scanning electron micrographs using the line intercept analysis of Mendelson [20]. Hardness of the sintered compacts was measured using a Vickers microindentor at a load of 1.96 N (200 g) applied for 10 s. Prior to indentation, the surface of the sample was polished to 3 μm surface finish. Average hardness value was taken from seven indents made for each sample and the maximum error obtained was found to be less than 5%.

3. Results and discussion

3.1. Powder characterisation

The measured amounts of Ca and P in the starting powder were determined as 37.27 and 17.44 wt% respectively. This gave a Ca/P weight ratio of 2.137 and a molar ratio of 1.67 ± 0.02. This value is in agreement with the ideal stoichiometric molar ratio value for pure HA of 1.667. The FT-IR spectrum of the as-received HA powder (see Fig. 1) revealed only reflections corresponding to HA phase. The presence of vibrations due to other impurity phases was not detected.

Other researchers have reported a Ca/P ratio ranging from 1.5 to 1.8 in other commercially available HA. This discrepancy in the reported Ca/P ratio could be attributed to the different batches of starting powder produced by different manufacturers [21].

The XRD trace of the starting HA powder is shown in Fig. 2. The peak broadening which can be observed in Fig. 2 is an indication of the presence of submicron crystallite in the powder [3,22]. The XRD analysis is in

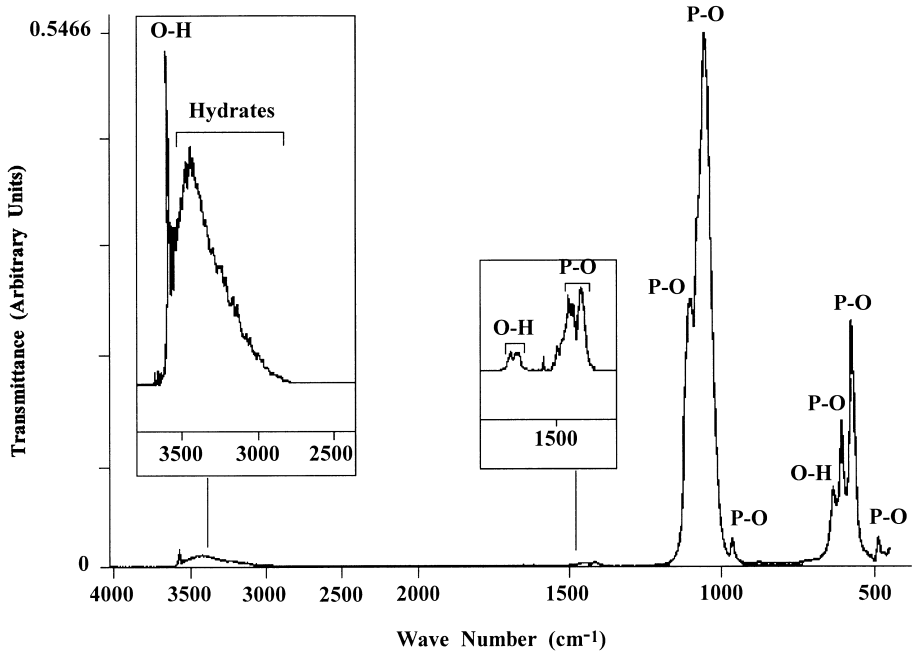

Fig. 1. IR absorption spectrum of commercial HA (Merck 2196) showing characteristic bands of O–H and P–O reflecting the vibrations of the OH and PO_4 in $Ca_{10}(PO_4)_6OH_2$.

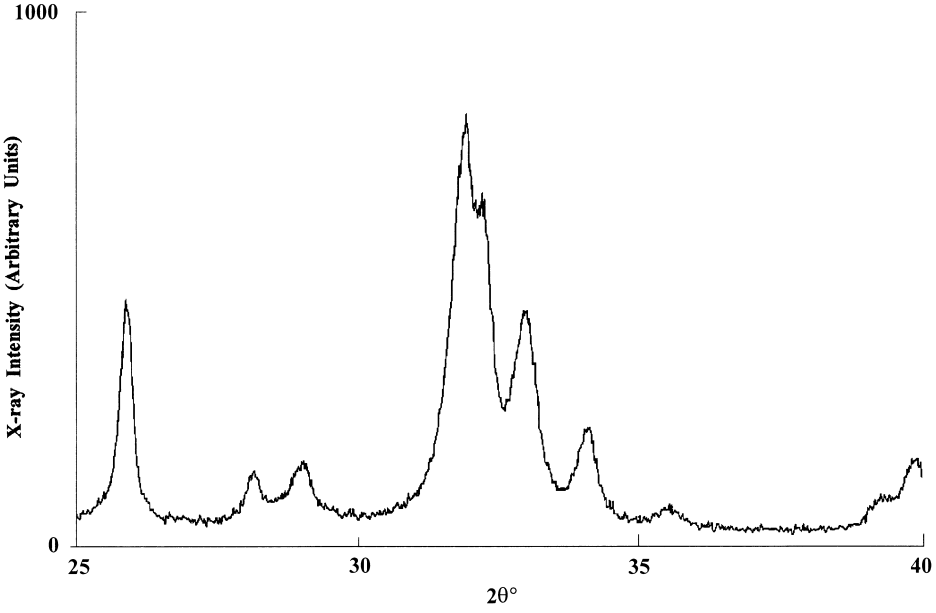

Fig. 2. XRD pattern of commercial HA powder at room temperature showing broad peaks which is believed to be due to the presence of submicron crystallites.

agreement with the FT-IR result which revealed that no other phases such as calcium carbonate or calcium oxide were present in the starting powder. Thus, from these results it can be inferred that the starting powder was highly crystalline and composed of pure HA particles.

Particle size distributions of the powder are shown in Fig. 3. The graph shows a broad range of particle sizes and appears to have a bimodal distribution. The average particle size was found to be ~10.6 μm while the median was ~6.2 μm. The surface area of the powder measured via BET technique was ~70 m^2/g. SEM micrographs of the powder (see Fig. 4) confirmed the presence of soft agglomerates that break up easily during compaction.

3.2. Phase stability

The result of phase analysis by XRD of the sintered samples is presented in Table 1. The X-ray diffraction

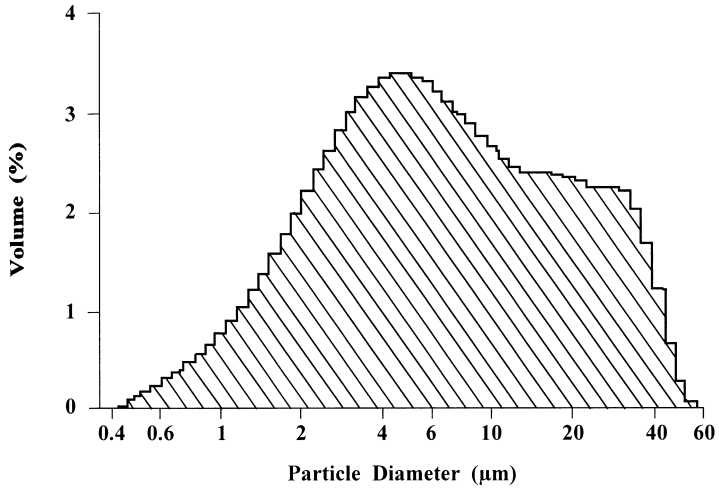

Fig. 3. Particle size distribution of the starting commercial hydroxyapatite powder. The presence of agglomerates is indicated by the secondary hump present from diameters 20–60 μm.

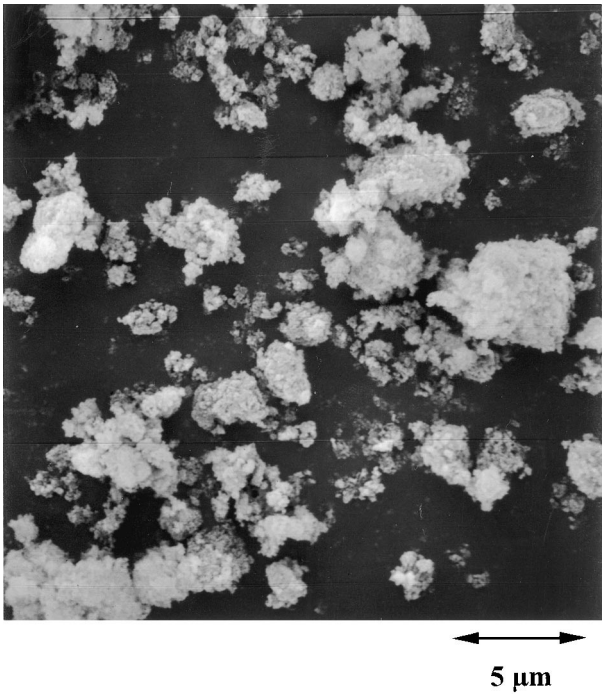

Fig. 4. Scanning electron micrograph of the commercial HA powder exhibiting the presence of soft agglomerates.

pattern of the samples sintered below 1350°C did not indicate the presence of any other phases other than HA, see Fig. 5.

Fig. 5(a) shows the pattern of a pure single phase material sintered at 1250°C with all peaks corresponding to the JCPDS card No. 9-432 for HA. X-ray diffraction patterns of samples sintered at 1400 and 1450°C are presented in Fig. 5(b) and (c) respectively. The former revealed the presence of α-TCP peaks indicating that HA has started to decompose at 1400°C. However, sintering at 1450°C resulted in further decomposition of HA to form β-TCP, TTCP and CaO.

Table 1
Phases detected at room temperature in the HA samples when sintered at various temperature

Sample	Sintering temperature (°C)	Phases detected by XRD
A-1	1000	HA
A-2	1050	HA
A-3	1100	HA
A-4	1150	HA
A-5	1200	HA
A-6	1250	HA
A-7	1300	HA
A-8	1350	HA
A-9	1400	HA, α-TCP
A-10	1450	HA, α-TCP, β-TCP, TTCP, CaO

In the present work, due to the fact that the Ca/P ratio was similar to the stoichiometric value, no other phases other than HA was detected when sintered up to 1350°C. Any deviation from the stoichiometric value would result in the formation of β-TCP in the samples when sintered <1350°C. Thus, the decomposition of HA at 1400°C in the present work, to form α-TCP, was not attributed to a non-stoichiometric HA.

However, it is believed that the decomposition of HA was associated with the formation of an intermediate phase, oxyapatite, that forms through gradual loss of the radical OH^- (dehydroxylation) in the matrix when HA is heated in air to above 1200°C. It has been suggested that during heating HA molecules tend to lose H_2O [18] and the formation of oxyapatite occurs according to the following equation [23,24]:

$$2OH \rightarrow O + H_2O \uparrow \quad (1)$$

$$Ca_{10}(PO_4)_6(OH)_2 \rightarrow Ca_{10}(PO_4)_6O{\cdot}\square + H_2O \quad (2)$$

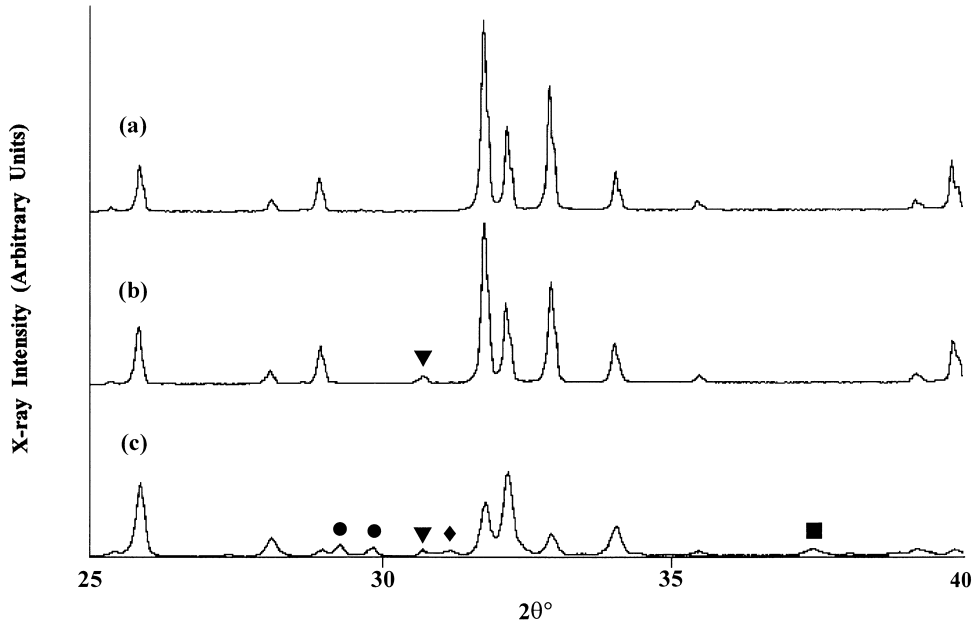

Fig. 5. X-ray diffraction patterns of HA sintered for 2 h at (a) 1250°C, (b) 1400°C and (c) 1450°C. (Key: ● = TTCP; ▼ = α-TCP; ◆ = β-TCP and ■ = CaO).

where □ is a non-charged vacancy and the hydroxyl-ion-deficient product $Ca_{10}(PO_4)_6O\cdot\square$ is known as oxyapatite [24]. Accordingly, one of the lattice sites which was originally occupied by two OH groups in a HA unit cell, is now occupied by an oxygen atom while leaving the other vacant. Zhou et al. [18] found that this oxyapatite phase is stable and will not undergo any reverse phase transformation. However, further heating, could lead to HA decomposition to form tricalcium phosphate and tetracalcium phosphate through the following process:

$$Ca_{10}(PO_4)_6(OH)_2 \rightarrow 2Ca_3(PO_4)_2 + Ca_4P_2O_9 + H_2O \quad (3)$$

The presence of CaO which was detected by XRD in the present material when sintered at 1450°C could be attributed to an alternative decomposition route according to the following reaction [25,26]:

$$Ca_{10}(PO_4)_6(OH)_2 \rightarrow 3Ca_3(PO_4)_2 + CaO + H_2O \quad (4)$$

In the present work, the HA samples were sintered in normal air atmosphere but degradation of the HA phase was only observed to occur in samples sintered $\geqslant$1400°C. Wang and Chaki [19] reported that decomposition of HA with a Ca/P ratio of 1.69 ± 0.01 started at 1100°C when sintered in air for 4 h. It is believed that the longer firing time employed by these authors could have facilitated dehydration process and promoted decomposition of HA to occur at lower temperature. However, Wang and Chaki found that when the sintering atmosphere was moisturised, the decomposition temperature could be increased >1300°C. In contrast, in the present work, all the samples were sintered in air for 2 h and decomposition of HA was only observed at higher temperatures. Therefore, it can be inferred that the high local humid atmosphere (i.e. the relative humidity is about 80% throughout the year) could have facilitated sintering by providing sufficient water vapour in the furnace atmosphere and preventing the decomposition of HA at temperatures <1400°C.

3.3. Relative density

The effect of sintering temperatures on the relative density and linear shrinkage of HA are shown in Fig. 6. It was found that the linear shrinkage increases from 22.2% at 1000°C to 30.2% at 1450°C with maximum shrinkage of 30.8% occurring at 1250°C. The relative density plot which showed an increase in measured density from 77.3% (sintered at 1000°C) to 98.5% (sintered at 1450°C) also exhibited a similar trend. The maximum density of >99% was measured for samples sintered between 1250 and 1400°C (see Fig. 6). These measured densities are high and are not in agreement with some of the values reported in the literature for HA ceramics sintered up to 1400°C [7,19,27]. These differences could be attributed to the history of the starting powder and processing thereafter.

In general, both the curves in Fig. 6 resemble very closely to each other, exhibiting a sigmoidal shape with an inflexion point around 1250°C. This point marks the temperature where maximum densification start to take place.

It can be noted from Fig. 6 that maximum densification did not occur until the sintering temperature was

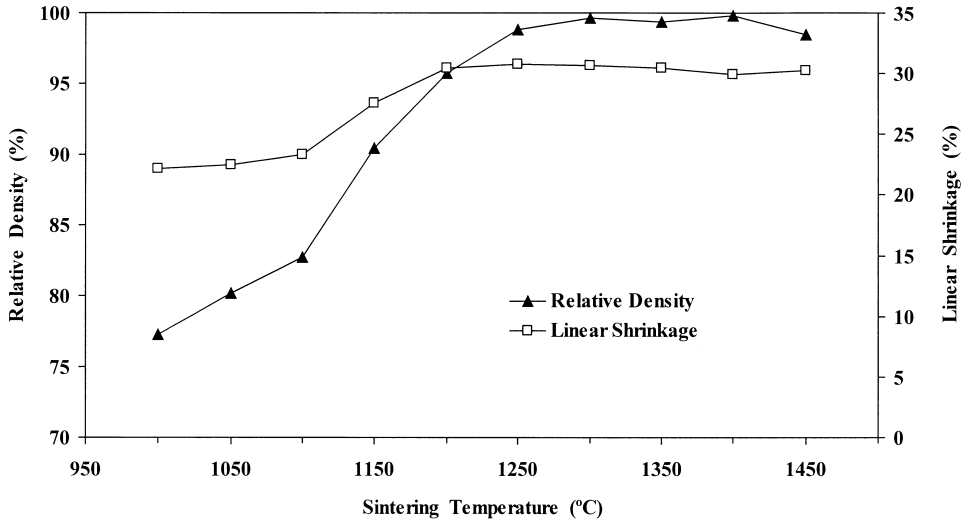

Fig. 6. The effect of sintering temperatures on the relative density and linear shrinkage of HA ceramics.

increased to 1200°C. SEM examination of samples sintered below 1200°C showed the presence of large pores which explained the low bulk density of this sample. However, as the sintering temperature was increased there was a gradual reduction in porosity (see Fig. 7). Samples sintered >1200°C gave a porosity level of less than 1%, indicating that sintering was almost complete. The pores present in these samples were mainly found to be located at grain boundaries. In contrast, the decrease in bulk density exhibited by samples sintered at 1450°C (see Fig. 6) could be attributed to the severe decomposition of HA as revealed in Fig. 5.

3.4. Microstructural evolution

Scanning electron micrographs (SEM) of the sintered samples are shown in Fig. 7. The samples sintered above 1200°C exhibited very little porosity as compared to those sintered at 1200°C and below.

In Fig. 8, the variation in average grain sizes with sintering temperature is presented. In general, the grain size increases slowly with sintering temperature up to 1250°C. However, as the temperature was increased >1250°C considerable grain growth occurred when compared to the sample fired at 1200°C. For instance, the average measured grain size of samples sintered at 1250 and 1400°C were 2.03 and 12.26 μm respectively.

At higher temperatures grain growth continues at an accelerated rate. The activation energy for grain growth was determined from the grain size measurements by constructing an Arrhenius plot for a constant sintering time as shown in Fig. 9. The best fit line was plotted by using the least min square method. The slope of this line was used to determine the activation energy (Q) from the following equation [28]:

$$D = A\exp[Q/RT] \quad (5)$$

where D is the average grain size, T is the temperature and R is the gas constant, i.e. 8.314 kJ/kmol K. The value for Q obtained from this plot for grain growth in hydroxyapatite was 58 kcal/mol. This value, which should correspond to the activation energy for diffusion in HA is in agreement with values reported by other researchers e.g. 47 kcal/mol [29], 56 kcal/mol [1] and 57 kcal/mol [25]. However, it should be noted that an activation energy value as low as 34 kcal/mol [6] has been reported which deviates significantly from the value obtained in the present work. This discrepancies in reported values could be attributed mainly to the different starting HA powder used and the sintering schedule employed.

3.5. Vickers hardness

The variation of the average Vickers hardness of samples sintered at various temperature is shown in Fig. 10. It can be noted that the lowest hardness value of 1.17 ± 0.073 GPa was measured for sample sintered at 1000°C, whereas the maximum hardness value of 6.08 ± 0.28 GPa was obtained for sample sintered at 1250°C. The general trend which can be observed from Fig. 10 is that the hardness increases slowly from 1000 to 1100°C and then increased rapidly, by a factor of more than 300%, when the temperature was increased from 1150 to 1250°C. However, further increase in temperature >1250°C resulted in a decrease in the hardness property. The measured hardness value for sample sintered at 1450°C was 4.53 ± 0.21 GPa.

The relatively low hardness obtained for samples sintered at temperatures <1200°C was not due to decomposition of HA but attributed to the low bulk density of the material. The relationship between grain size, relative density and hardness are shown in Fig. 11. It can be noted that below ~2 μm the hardness trend correlates

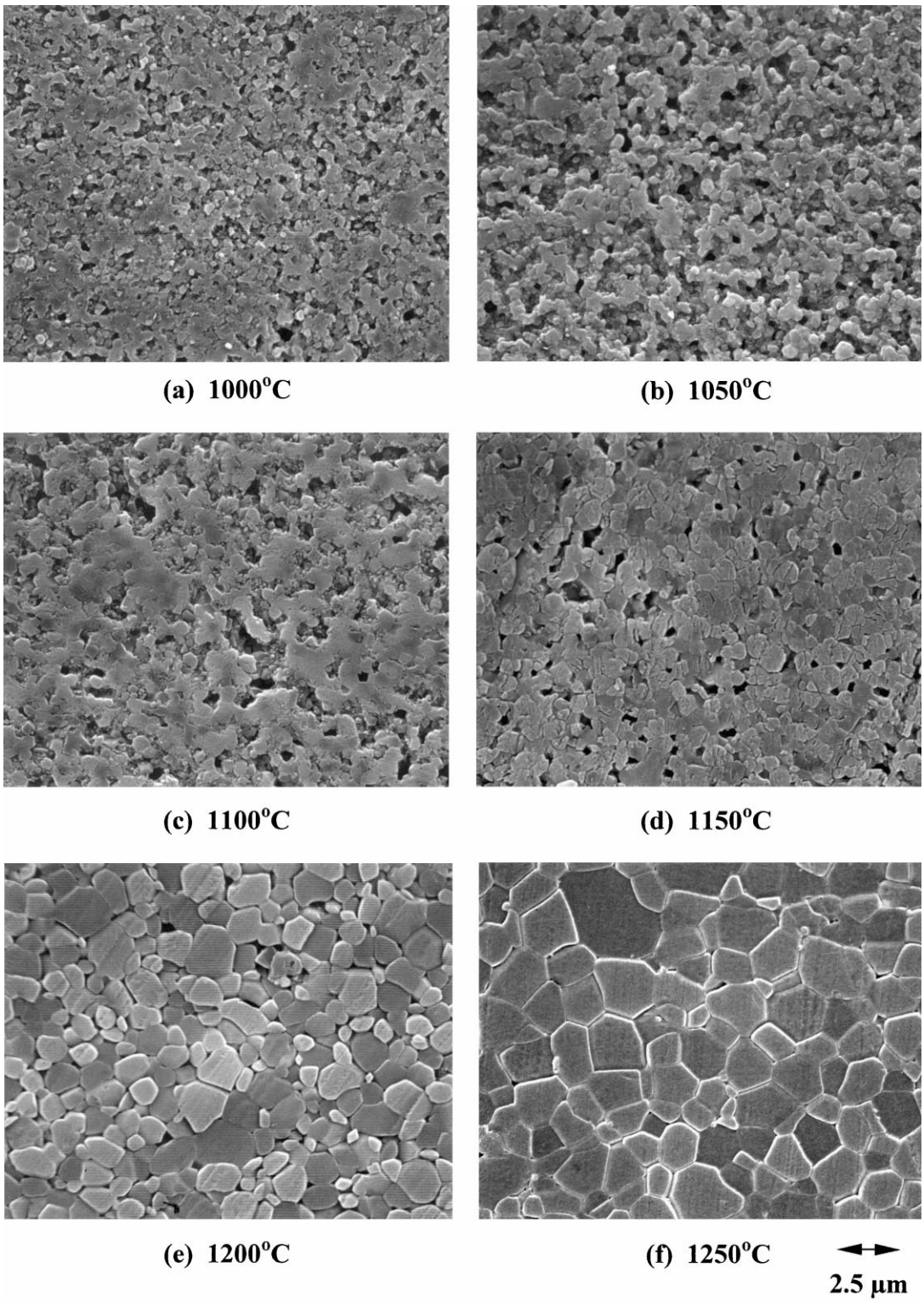

Fig. 7. SEM micrographs of polished and etched HA surface sintered at various temperatures.

well with the change in relative density i.e. hardness increases steadily with relative density (see Fig. 11). However, above 2 μm the variation in hardness seem not to be in agreement with the density curve. i.e. the relative density was found to remain constant >98–99% while the hardness gradually decreased with increasing grain size. Therefore it is hypothesised that below some critical grain size e.g. (d_c) the hardness is governed by bulk density (or porosity). In contrast, above d_c (e.g. in this work $d_c = \sim 2$ μm) the bulk density is not the controlling parameter but rather grain growth.

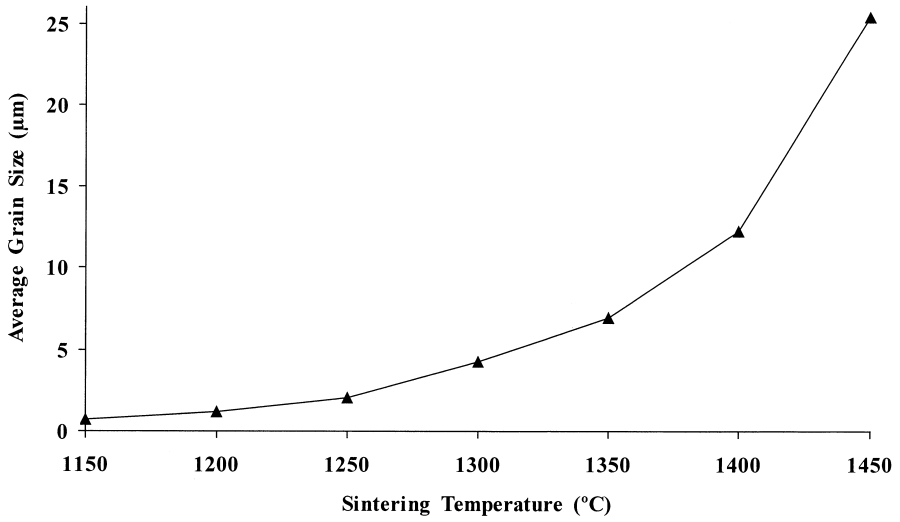

Fig. 8. The effect of sintering temperature on the average grain size of HA.

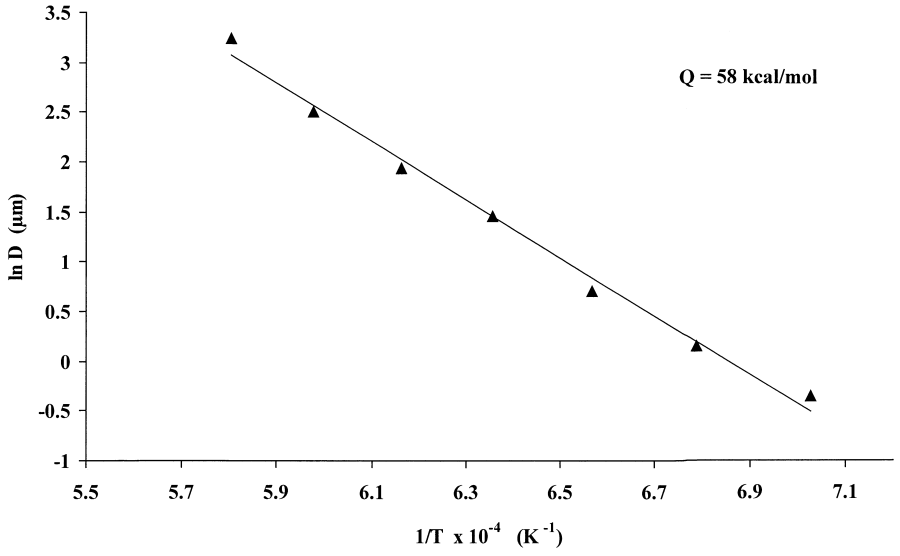

Fig. 9. Arrhenius plot of log mean grain size against reciprocal of sintering temperature for polycrystalline HA.

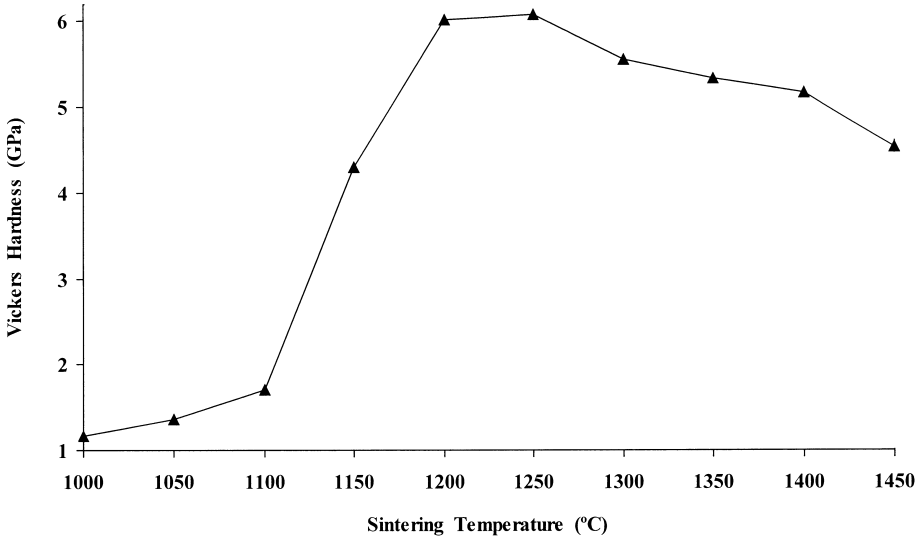

Fig. 10. Vickers hardness values of HA sintered at a range of temperatures.

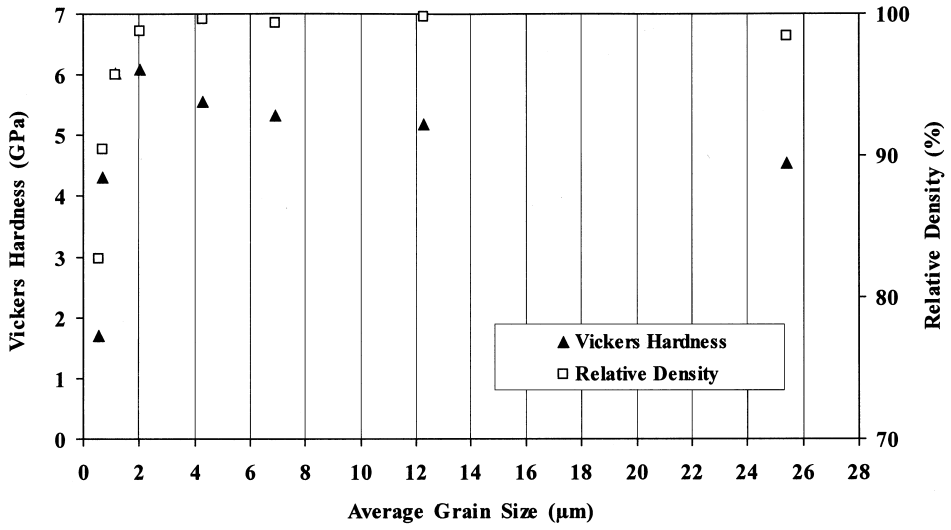

Fig. 11. Variation of Vickers hardness and relative density as a function of average grain size.

Another factor which could have, in part, contributed to the decline in hardness after sintering at elevated temperatures >1400°C is the decomposition of HA which would have hindered the formation of strong inter-particle bonding in the ceramic matrix. Jarcho et al. [1] have reported the presence of decomposition products at grain boundaries of HA sintered in air at 1250°C for 1 h. Wang and Chaki [17] have also agreed that the degradation of mechanical properties in HA was due to weakening of the grain boundary as a result of segregation of decomposition product at grain boundary regions. Therefore, based on these observations and the results obtained in the present work, it can be inferred that both the presence of secondary phases and larger grain sizes are detrimental to densification and hardness.

4. Conclusions

1. In the present study, the results showed that the sintering temperature is a critical factor influencing the phase stability, densification behaviour, sintered microstructure and hence the hardness of hydroxyapatite ceramics.
2. The optimum sintering temperature for HA was found to be 1250°C. The measured properties at this temperature were as follows: bulk density of >99% dense and has an average grain size of about 2 μm. Maximum hardness value of 6.08 GPa was also measured for samples sintered at 1250°C.
3. As would be expected, sintering at lower temperatures (<1250°C) resulted in lower density. In contrast, the decrease in density with increasing temperature >1400°C was attributed to grain growth phenomenon and severe decomposition of HA phase.
4. The stability of HA phase in the sintered body was found to be dependent on the sintering temperature. Decomposition of HA was observed to occur in samples sintered above 1350°C.
5. There is a definite correlation between hardness and grain size. It is suggested that a certain critical grain size phenomenon was influencing the hardness of HA ceramics i.e. above this critical grain size, the hardness would decrease as a result of grain growth.
6. It has been shown in the present work that decomposition of HA was detrimental to sintering, densification and hardness property.

Acknowledgements

This work was supported under the IRPA grant No. 09-01-01-0014. The authors gratefully acknowledge the support provided by SIRIM Berhad, in particular, Dr. Mustaza Hj. Ahmadun of AMREC and Ms. Wan Zaharah of Ceramics Technology Centre. Thanks are also due to Ms. Zalena Saem for preparing the samples for SEM examination and Dr. S. Best (IRC in Biomedical Materials, Queen Mary and Westfield College, University of London) for her suggestion and time in reading this manuscript.

References

[1] M. Jarcho, C.H. Bolen, M.B. Thomas, J. Bobick, F. Kay, R.H. Doremus, J. Mater. Sci. 11 (1976) 2027.
[2] H. Akoi, K. Kato, M. Ogiso, T. Tabata, J. Dental Outlook 49 (1977) 567.

[3] H.S. Liu, T.S. Chin, L.S. Lai, S.Y. Chiu, K.H. Chung, C.S. Chang, M.T. Chang, Ceram. Int. 23 (1997) 19.
[4] K.A. Khor, P. Cheang, J. Mater. Proc. Technol. 63 (1997) 271.
[5] K.A. Khor, P. Cheang, Y. Wang, JOM 49 (1997) 51.
[6] G. De With, J.A. Van Dijk, H.N. Hattu, K. Prijs, J. Mater. Sci. 16 (1981) 1592.
[7] M. Akao, H. Aoki, K. Kato, J. Mater. Sci. 16 (1981) 809.
[8] M. Ogiso, N. Nakabayashi, T. Matsumoto, M. Yamamura, R.R. Lee, J. Biomed. Mater. Res. 30 (1996) 109.
[9] S. Best, W. Bonfield, J. Mater. Sci.: Mater. in Med. 5 (1994) 516.
[10] R. Legeros, Clin. Mater. 14 (1993) 65.
[11] S.I. Stupp, G.W. Ciegler, J. Biomed. Mater. Res. 26 (1992) 169.
[12] R.G.T. Geesink, K. De Groot, P.A.T. Christel, Clin. Orthop. 225 (1987) 147.
[13] R.G.Y. Geesink, K. De Groot, C.P.A. Klein, J. Bone Joint Surf. 70B (1988) 17.
[14] B. Kellett, F.F. Lange, J. Am. Ceram. Soc. 67 (1984) 369.
[15] G. Muralithran, S. Ramesh, Internal report No. 09-01-01-0014-01, SIRIM Berhad, 1997.
[16] A. Tampieri, G. Celotti, F. Szontagh, E. Landi, J. Mater. Sci.: Mater. in Med. 8 (1997) 29.
[17] L.L. Hench, J. Wilson, in: An Introduction to Bioceramics. World Scientific, 1993, pp. 152.
[18] J. Zhou, X. Zhang, J. Chen, S. Zeng, K. De Groot, J. Mater. Sci.: Mater. in Med. 4 (1993) 83.
[19] P.E. Wang, T.K. Chaki, J. Mater. Sci. Mater. in Med. 4 (1993) 150.
[20] M.I. Mendelson, J. Am. Ceram. Soc. 52 (1969) 443.
[21] S. Best, B. Sim, M. Kayser, S. Downes, J. Mater. Sci.: Mater. in Med. 8 (1997) 97.
[22] L. Dean-Mo, J. Mater. Sci.: Mater. in Med. 8 (1997) 227.
[23] A. Krajewski, A. Ravaglioli, Bioceramics 5 (1984) 105.
[24] T. Kijima, M. Tsutsumi, J. Am. Ceram. Soc. 62 (1979) 455.
[25] K. Kamiya, T. Yoko, K. Tanaka, Y. Fujiyama, J. Mater. Sci. 24 (1989) 827.
[26] J. Wu, T. Yeh, J. Mater. Sci. 23 (1988) 3771.
[27] M. Toriyama, A. Ravaglioli, A. Krajewski, G. Celotti, A. Piancastelli, J. Eur. Ceram. Soc. 16 (1996) 429.
[28] R.E. Smallman, R.J. Bishop, in: Metals and Materials: Science, Processes, Applications. Butterworth-Heinemann Ltd., Oxford, 1995, pp. 83.
[29] P. Van Landuyt, F. Li, J.P. Keustermans, J.M. Streydio, F. Delannay, E. Munting, J. Mater. Sci.: Mater. in Med. 6 (1995) 8.